Korean J. Chem. Eng., **30**(10), 1960-1965 (2013)
DOI: 10.1007/s11814-013-0126-4

Effect of cysteamine layer on the interaction between gold and ZrO_2 surfaces

Jin-Won Park†

Department of Chemical and Biomolecular Engineering, College of Energy and Biotechnology,
Seoul National University of Science and Technology, 172, Gongreung2-dong, Nowon-gu, Seoul 139-743, Korea
(*Received 12 March 2013 • accepted 10 July 2013*)

Abstract−The formation of cysteamine layer on gold surfaces may have an effect on the distribution of either gold particle adsorbed to the ZrO_2 surface or vice versa with the adjustment of the electrostatic interactions. The atomic force microscope (AFM) was used to measure the surface forces between the zirconia surface and the cysteamine surface s as a function of the salt concentration and pH value. With the Derjaguin-Landau-Verwey-Overbeek (DLVO) theory, the forces were quantitatively analyzed to acquire the surface potential and charge density of the surfaces for each salt concentration and each pH value. The surface potential and charge density dependence on the salt concentration was described with the law of mass action, and the pH dependence was explained with the ionizable groups on the surface.

Key words: Cysteamine, Gold Surface, ZrO_2 Surface, AFM, DLVO Theory

INTRODUCTION

Materials composed of gold and a semiconducting support such as ZrO_2 may be useful for various applications, such as in surface patterning, hydrogenation, and CO oxidation [1-4]. In the latter case, the excitation of the semiconductor-metal nanocomposite by CO adsorption may be utilized for the activation of oxygen, i.e., for the production of carbon dioxide by oxygen splitting [5]. Activity and selectivity of such materials and catalysts rely on the distribution [6].

Different methodologies have been developed to prepare Au-Oxide catalyst materials such as metal ion impregnation and deposition-precipitation followed by drying, calcinations, and reduction [7-9]. During such procedures, the Au particles or clusters are deposited directly on the support. However, these methodologies have several disadvantages. Polydispersity of the resulting metal particles is generated due to the uneven precursor-solution loading caused by gravitational forces. The necessary thermal treatment furthermore results in severe agglomeration problems and may even induce chemical modification of the support through ionic diffusion [6]. Therefore, an alternative approach has been considered for catalyst preparation [10]. A different approach is involved in the preparation of metallic Au^0 particles in solution and subsequent deposition on the oxide. This approach is based on passivating ligands such as phosphines and thiols [11,12]. This methodology prevents the particles from agglomeration. After the gold particles or cluster are formed on the oxide, the ligands can be removed by calcinations of the material and thiolate oxidation [13-15].

The atomic force microscope (AFM) provides a useful means to measure directly the total force of interaction between a colloidal particle and a flat surface as a function of separation [16]. The analysis of these separation-force curves with Derjaguin-Landau-Verwey-Overbeek (DLVO) theory is capable of acquiring the electrostatic surface properties of the surface being studied [17]. These surface properties are an indicator to represent electrostatic repulsive force between particles, which may strongly affect the particle distribution that the activity and selectivity of the catalysts depend on. Therefore, they have been characterized for gold and ZrO_2 surfaces which were coated with several materials [18-23]. We investigated the effect of the cysteamine layer formation on gold surfaces interacting with the ZrO_2 surfaces.

EXPERIMENTAL

1. Surface Preparation

The gold surfaces were prepared by sequential deposition of a 5 nm chrome adhesion layer and a 100 nm gold layer on the silicon wafers using a high-vacuum electron beam evaporator. Immediately prior to use, the gold surfaces were cleaned in a 4 : 1 solution of 96% sulfuric acid and 30% hydrogen peroxide at 60-80 °C for 5 min. The gold surface was immersed in a solution of 10 mM cysteamine, 100 mM potassium nitride, at pH 4 for several hours at room temperature, followed by rinsing with a running buffer. The successful immobilization of cysteamine layer was clearly found from qualitative surface force measurement in 100 mM potassium nitride at pH 4. For quantitative surface force measurements, the solution was replaced with a running buffer (there are six running buffers used in this research - 100, 10, and 1 mM potassium nitride at pH 4 and 8, respectively). ZrO_2 layer was deposited on the surface of the silicon wafer by sputtering zirconium in an argon-oxygen environment for 41 min using an RF Magnetron source operating at 2 kW. Prior to sputtering, the wafers were dipped in hydrofluoric acid to remove any native oxide layer. The total pressure used was 5×10^{-6} bar, with argon and oxygen flow rates of 6 and 1.2 dm^3/min, respectively. The wafers were rotated continuously during sputtering. The target to wafer distance was 20 cm and target diameter was 7 cm. The characteristics of the ZrO_2 layers were identical to those of the gold surface.

2. AFM Measurements

Topology images and surface force measurements were made

†To whom correspondence should be addressed.
E-mail: jwpark@seoultech.ac.kr

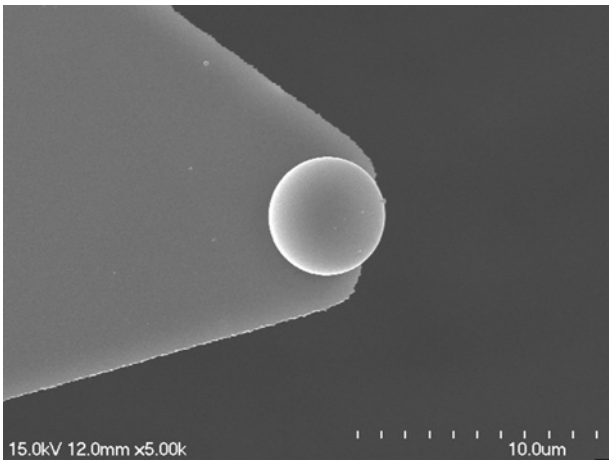

Fig. 1. Zirconium dioxide sphere-attached-cantilever.

with a 3-D Molecular Force Probe AFM (Asylum Research, Santa Barbara, CA) with a closed-loop piezo-electric transducer. Microfabricated silicon oxynitride cantilevers (Olympus, Shinjuku-ku, Tokyo, Japan) with a nominal radius of 20 nm were used for topographic imaging and qualitative surface force measurements. Quantitative surface force measurements were made with zirconium oxide spheres (Microspheres-Nanospheres, Cold Spring, NY) of 3 μm diameter that were attached to the microfabricated cantilevers, shown in Fig. 1. The sphere was immobilized at the end of the cantilever using UV-sensitive adhesive (Norland Products, New Brunswick, NJ). Exposure to the UV light source and surface cleaning were achieved in an ozone generating UV-apparatus (Jelight, Irvine, CA). It was confirmed that the exposure did not cause any change in the response of the cantilever. The spring constant of the cantilever was estimated using the thermal frequency spectrum of the cantilever [24].

X-ray photoelectron spectra (XPS) were obtained with a spectrometer equipped with a concentric hemispherical analyzer (SSX301 x-ray photoelectron spectrometer, Surface Science Instruments). The instrument was operated in a fixed analyzer transmission mode using a monochromatic x-ray source. The pass energy was 50 eV with a 300 μm spot size, the take-off angle was 35°, and the normal operating pressure was 10^{-9} Torr.

THEORY

The Derjaguin-Landau-Verwey-Overbeek (DLVO) theory is well known as the description for the forces between interacting electrostatic double layers which have been considered by numerous authors [25]. According to the theory, the total interaction energy between two plates can be considered as the sum of several contributions, including an attractive van der Waals component (V_A) and an electrostatic repulsion or attraction (V_E). There is also considerable evidence for an additional repulsion (V_S) at close separations resulting from the presence of ordered solvent layers [26-29].

According to the Derjaguin approximation, the force between sphere of radius R_T and a plate can be interpreted into the energy between plates by the expression [30]

$$F/R_T=2\pi(V_A+V_E+V_S) \quad (1)$$

The van der Waals energy (V_A) in the non-retarded limit is described by an equation of the form

$$V_A=-A_H/12\pi d^2 \quad (2)$$

where A_H is the Hamaker constant and d is the separation distance [31]. For the cysteamine layer, the Hamaker constant is assumed to be 7.0×10^{-20} J, because the most component of the layer is hydrocarbon [32]. The Hamaker constant used for the ZrO_2 surface is 10.0×10^{-20} J [33]. The electrostatic interaction (V_E) can be derived by either considering the free energy associated with the formation of a double layer or by integrating the electrostatic force [34-36]. The interaction for a 1 : 1 electrolyte is

$$V_E=-\int_{\infty}^{D}\left\{2n^0kT\left[\cosh\left(\frac{ze\psi}{kT}\right)-1\right]-\frac{\varepsilon}{2}\left(\frac{d\psi}{dz}\right)^2\right\}dz \quad (3)$$

where ψ is the electrostatic potential. The first term in Eq. (3) is a repulsive osmotic component from the accumulation of charge between the plates, and the second is a Maxwellian stress that means an induced charge and is always attractive. For similarly charged surfaces, the second term disappears, leaving a results equivalent to DLVO. To calculate V_E, ψ must be found first. The potential can be acquired from the solution of the Poisson-Boltzmann equation,

$$\frac{d^2\psi}{dz^2}=-\frac{1}{\varepsilon_0\varepsilon_r}\sum_i n_i^0 z_i e\exp\left(-\frac{z_i e\psi}{kT}\right) \quad (4)$$

Generally, the complete nonlinear form of Eq. (4) must be solved, which can be accomplished only by numerical techniques [37]. Eq. (3) was integrated with Simpsons' 3/8 rule. The additional repulsive energy (V_S) in Eq. (1) is thought to arise from the presence of ordered solvent layers and can be described by a decaying oscillatory force [38]. The nature of this repulsive force is not clearly understood and will be neglected in the calculations presented here.

RESULTS AND DISCUSSION

The AFM was used to characterize the structures of the cysteamine layer formed on the gold surfaces. Constant force AFM images were obtained on the gold surfaces, cysteamine-coated gold surfaces, and ZrO_2 surfaces. The morphologies of the gold surfaces, the cysteamine-coated gold surface, and the ZrO_2 surfaces were dominated by the polycrystalline structure of the evaporated metals and had a roughness of 1.5 nm. Again, the morphologies of these surfaces were essentially indistinguishable (results not shown). Phase separation in lipid and fatty acid films has been found with AFM and is easily visualized as micrometer-sized domains in the constant force AFM images [39]. The domains were not observed on the cysteamine-coated gold surfaces, and no observation means that the cysteamine forms homogeneous layer on the gold surfaces.

AFM force measurements were performed on the gold surfaces and the cysteamine-coated gold surfaces with 20-nm-radius probes to confirm the formation of cysteamine layer on the gold surfaces. Fig. 2 presents approaching force-distance curves between a silicon nitride probe in 100 mM potassium nitride at pH 4. The observed forces on the cysteamine layer were purely short-range-repulsion below around 2.0 nm at loads of approximately 0.2 nN, while the force curve of the gold surface had an attractive region. The repulsion, not observed on the gold surfaces, appears to be caused by

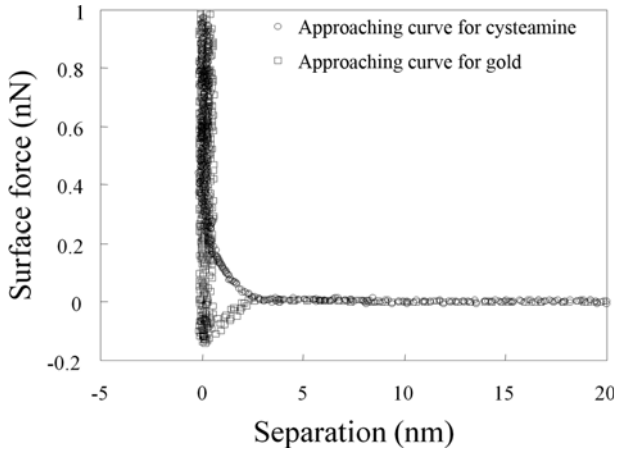

Fig. 2. Force-distance curve between a silicon nitride probe and the cysteamine layer formed in 100 mM potassium nitride at pH 8.0.

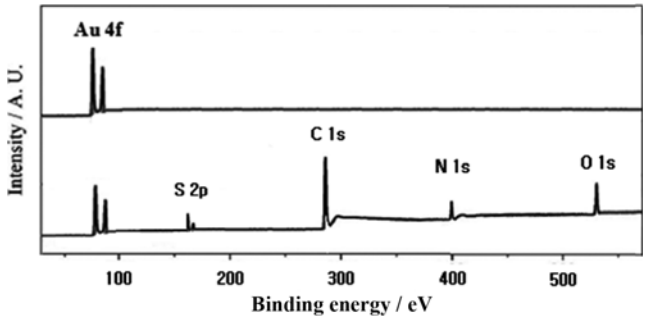

Fig. 3. Results of XPS study for the formation of the cysteamine layer. The top graph is for the Au surface without the immersion, and the bottom is for the surface with the immersion.

the lower Hamaker constant and more hydration of the cysteamine layer [38]. The clear difference of the force curve suggests that the cysteamine layers were formed on the gold surfaces. The formation of the cysteamine layer was also confirmed using XPS data. The results are shown in Fig. 3. The graph on top is for the Au surface without the immersion, and the graph at the bottom is for the surface with the immersion. As shown, the immersion has caused a change

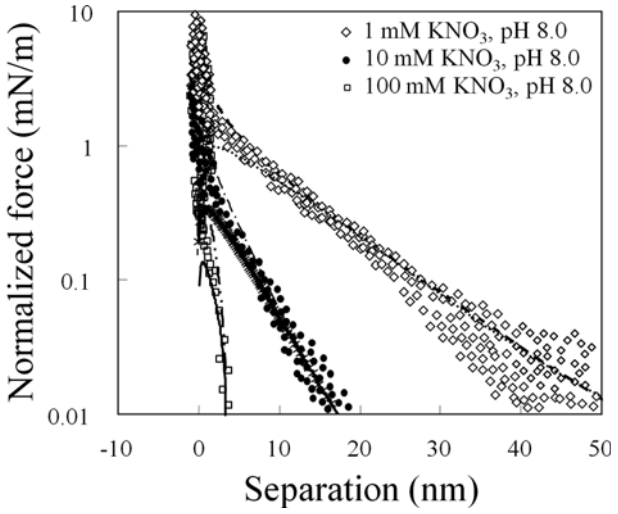

Fig. 4. Approaching force curve as a function of the separation between the sphere and the surface of the zirconium dioxide in 1, 10, 100 mM potassium nitride at pH 8.0.

in the peaks, especially S, C, N atoms that are the components of the cysteamine.

For the quantitative characterization of the cysteamine-coated-gold surface properties, the surface charge density and potential of the 3-μm-diameter zirconium dioxide sphere were acquired as a first with the force measurements between the sphere and the zirconium dioxide surface. Fig. 4 shows the approaching surface force curves as a function of the separation between the zirconium dioxide sphere and the zirconium dioxide surface in three running buffers at pH 8. The long-range surface forces were purely repulsive, and their range was highly dependent on the ionic strength of the solution. The exponential dependence of the repulsive force on distance was consistent with the double-layer forces between surfaces of like charge in aqueous solutions. At the separations of less than around 2 nm, additional repulsive-forces were observed that may be attributed to the steric forces and the inherent roughness of the surfaces [40,41].

However, the behavior of the long-range surface forces at pH 4 was different from those at pH 8. The range of the repulsive forces, observed in 1 mM potassium nitrate solution at pH 4, was around 10 nm that was much shorter than that at pH 8 due to the iso-electric

Table 1. Electrostatic properties of the zirconium dioxide surfaces

	pH 8		
	1 mM Potassium nitrate	10 mM Potassium nitrate	100 mM Potassium nitrate
Surface potential (mV)	−40±4	−26±3	−17±2
Surface charge density (10^{-3} C/m^2)	−2.8±0.3	−6.5±0.6	−11.5±1.3
	pH 4		
	1 mM Potassium nitrate	10 mM Potassium nitrate	100 mM Potassium nitrate
Surface potential (mV)	+10.3±1	-*	-*
Surface charge density (10^{-3} C/m^2)	+0.8±0.2	-*	-*

*Electrostatic property was not acquired

point of ZrO_2. The forces were not found in 10 mM and 100 mM potassium nitrate solution at pH 4. In other words, in 10 mM and 100 mM potassium nitrate solution at pH 4, the electrostatic forces in the long range appeared not to be the dominant component of the surface forces on the ZrO_2 surface. Therefore, in 10 mM and 100 mM potassium nitrate solution at pH 4, it was not appropriate to analyze the force curves with the DLVO theory so that the surface potential and charge density could not be acquired.

The long-range surface forces were analyzed with the DLVO theory to estimate either constant surface potential or constant surface charge density, as the fitting curves shown in Fig. 4. The results of this analysis are summarized in Table 1. The surface potential of the zirconium dioxide surface is on the order of −10 to −100 mV at pH 8.0. Our results appear to be consistent with those of Choi et al., where electrophoretic technique was used to characterize the charge state of the zirconium dioxide surface [42]. The change from negative potential to positive potential is due to change from negative to positive values at an isoelectric point of pH 5.5 [43]. For the 10 mM and 100 mM potassium nitrate solution at pH 4, the surface potential and charge density of the ZrO_2 were not estimated.

As shown in Table 1, the surface potential of the zirconium dioxide surface increased monotonically with decreasing ionic strength, and the surface charge density deceased monotonically with decreasing ionic strength at pH 8. Pashley developed a model to explain the salt concentration dependence of the surface potential and charge density of a surface with ionizable groups based on the law of mass action [44]. The relation between surface charge density (σ), surface potential (ψ_o), and salt concentration may be found by the simultaneous solution of the law of mass action,

$$\sigma = \sigma_o \frac{1}{1 + K_a[H^+]\exp\left(-\frac{e\psi_o}{kT}\right) + K_{K^+}[K^+]\exp\left(-\frac{e\psi_o}{kT}\right)} \quad (5)$$

and Graham's equation,

$$\sigma = \sqrt{8\varepsilon\varepsilon_o kT}\sinh\left(\frac{e\psi_o}{kT}\right)\sqrt{([K^+]+[H^+])} \quad (6)$$

where σ_o is the maximum surface charge density, ψ_o is the surface potential, ε is the dielectric constant of water, ε_o is the permittivity of free space, e is the electronic charge constant, k is the Boltzmann's constant, T is temperature. The dependence of surface potential and charge density on the salt concentration, found at pH 8, was consistent with the prediction from Pashley's model. For the purpose of this study, the experimentally measured zirconium dioxide surface potential and charge density were used to characterize the cysteamine layer formed on the gold surfaces.

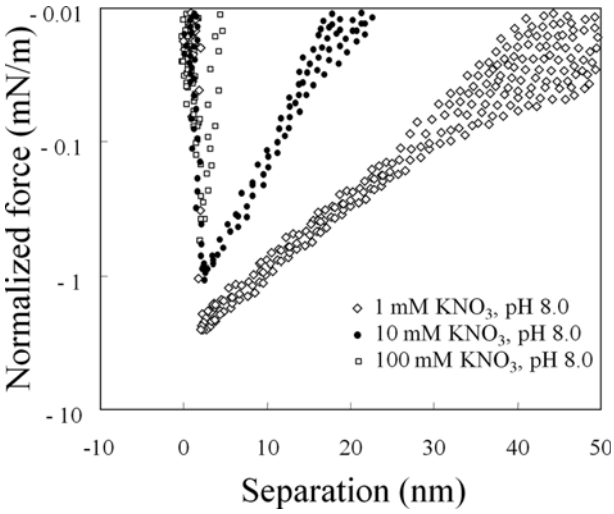

Fig. 5. Approaching force curve as a function of the separation between the zirconium dioxide sphere and the cysteamine layer in 1, 10, 100 mM potassium nitride at pH 8.0.

The surface potential and charge density of the cysteamine layer formed on the gold surfaces were characterized from analyzing with the DLVO theory the long-range surface force measured on them with the zirconium dioxide sphere. Fig. 5 shows the results of force measurements made on the cysteamine layers in the three running buffers at pH 8. The long-range surface forces were purely attractive and varied in range with ionic strength in a manner that was consistent with double-layer forces. Quantitative analysis of the surface forces was performed with the DLVO theory at asymmetric boundary conditions. Table 2 summarizes the surface potentials and charge densities measured on the cysteamine layers as a function of ionic strength and pH value. The surface potential and charge density dependence of the cysteamine layer on the salt concentration were also consistent with Pashley's model. It was observed that the surface charge densities and potentials of the cysteamine layer

Table 2. Electrostatic properties of the cysteamine layer

	pH 8		
	1 mM Potassium nitrate	10 mM Potassium nitrate	100 mM Potassium nitrate
Surface potential (mV)	+78±7	+40±5	+26±3
Surface charge density (10^{-3} C/m^2)	+13±2	+22±3	+45±5
	pH 4		
	1 mM Potassium nitrate	10 mM Potassium nitrate	100 mM Potassium nitrate
Surface potential (mV)	-**	-**	-**
Surface charge density (10^{-3} C/m^2)	-**	-**	-**

**Electrostatic property was not acquired

had different sign compared to those for the zirconium dioxide surfaces at pH 8, which can be attributed to the ionized-functional-groups of the cysteamine layer. The long range forces were not found in 1 mM potassium nitrate solution at pH 4. This phenomenon was predictable, considering pK_a of the cysteamine and the iso-electric point of ZrO_2. The long range forces were not observed in 10 mM and 100 mM potassium nitrate salt concentrations at pH 4, either. This observation was consistent with the long-range forces not observed on the ZrO_2 surfaces.

The results described above suggest that the electrostatic forces between the cysteamine-coated gold surfaces and ZrO_2 surfaces were found to be adjustable quantitatively with a salt concentration and pH value. In the previous researches, the electrostatic properties of the cysteamine coating were adjusted with pH [45,46]. Therefore, it was thought that the kinetics of the adsorption for either ZrO_2 particles to cysteamine-coated-gold surface or cysteamine-coated-gold particles to ZrO_2 surface might be also adjustable, because the adsorption is determined by the surface forces between the surfaces. Furthermore, the kinetics has an effect on the distribution of the particles adsorbed to the surface. Therefore, the surface forces as a function of the salt concentration and the pH value seem to be important for the design of the distribution of the particles adsorbed to the surfaces, which can affect on the efficiency of catalysts.

In conclusion, the surface forces between the cysteamine-coated-gold surface and the ZrO_2 surface were measured as a function of the salt concentration and pH value using the AFM. By applying the DLVO theory to the long-range surface forces, the surface potential and charge density of the surfaces were quantitatively acquired for each salt concentration and each pH value. The surface potential and charge density dependence on the salt concentration was explained with the law of mass action, and the pH dependence was with the ionizable groups on the surface. The electrostatic properties between the cysteamine-coated-gold surface and the ZrO_2 surface have not been quantitatively made so far, although the properties may be fundamental to adjust the distribution of the ZrO_2 domain on the gold surface or vice versa. From this study, it was suggested that the coating cysteamine on gold surfaces may be used to design the distribution of either gold particle adsorbed to the ZrO_2 surface or vice versa by adjusting the electrostatic interactions.

ACKNOWLEDGEMENTS

This study was financially supported by Seoul National University of Science and Technology. We thank all of members of the Department of Chemical and Biomolecular Engineering, the Seoul National University of Science and Technology for help and valuable discussions.

REFERENCES

1. D. M. Soolaman and H.-Z. Yu, *J. Phys. Chem. C*, **111**, 14157 (2007).
2. H. Pu, L. Zhang, D. Du, C. Han, H. Li, J. Li and Y. Luo, *Korean J. Chem. Eng.*, **29**, 1285 (2012).
3. X. Zhang, H. Shi and B.-Q. Xu, *J. Catal*., **279**, 75 (2011).
4. C.-M. Wang, K.-N. Fan and Z.-P. Liu, *J. Am. Chem. Soc.*, **129**, 2642 (2007).
5. S. Arrii, F. Morfin, A. J. Renouprez and J. L. Rousset, *J. Am. Chem. Soc*., **126**, 1199 (2006).
6. X. Zhang, H. Wang and B. Q. Xu, *J. Phys. Chem. B*, **109**, 9678 (2005).
7. P. V. Kamat, *J. Phys. Chem. C*, **111**, 2834 (2007).
8. M. Valden, X. Lai and D. W. Goodman, *Science*, **281**, 1647 (1998).
9. H. Sakurai, S. Tsubota and M. Haruta, *Appl. Catal. A-Gen.*, **102**, 125 (1995).
10. X. Li, J. Fu, M. Steinhart, D. H. Kim and W. Knoll, *Bull. Korean Chem. Soc.*, **28**, 1015 (2008).
11. G. Schmid, *Chem. Rev.*, **92**, 1709 (1992).
12. J. Noh, H. Park, Y. Jeong and S. Kwon, *Bull. Korean Chem. Soc.*, **27**, 403 (2006).
13. M. Dasog and R. W. J. Scott, *Langmuir*, **12**, 3381 (2007).
14. N. Sandhyarani and T. Pradeep, *Chem. Phys. Lett.*, **338**, 33 (2001).
15. N. J. Brewer, R. E. Rawsterne, S. Kothari and G. J. Leggett, *J. Am. Chem. Soc.*, **123**, 4089 (2001).
16. G. Binnig, C. Quate and G. Gerber, *Phys. Rev. Lett.*, **56**, 930 (1986).
17. B. V. Derjaguin and L. Landau, *Acta Physiochem.*, **14**, 633 (1941).
18. M. Wisniewska, *Adsorp. Sci. Technol*., **24**, 673 (2006).
19. E. D. Kafuman, J. Belyea, M. C. Johnson, Z. M. Nicholson, J. L. Ricks, P. K. Shah, M. Bayless, T. Pettersson, Z. Feldoto, E. Blomberg, P. Claesson and S. Franzen, *Langmuir*, **23**, 6053 (2007).
20. E. A. Sanches, J. C. Soares, R. M. Iost, V. S. Marangoni, G. Trovati, T. Batista, A. C. Mafud, V. Zucolotto and Y. P. Mascarenhas, *J. Nanomater.*, 697071 (2011).
21. Z. J. Wang, J. H. Yuan, M. Zhou, L. Niu and A. Ivaska, *Appl. Surf. Sci*., **254**, 6289 (2008).
22. I. W. Lenggoro, H. M. Lee and K. Okuyama, *J. Colloid Interface Sci*., **303**, 124 (2006).
23. W. M. Huang and J. L. Shi, *J. Sol-Gel Sci. Technol*., **20**, 145 (2011).
24. J. P. Cleveland, S. Manne, D. Bocek and P. K. Hansma, *Rev. Sci. Instrum.*, **64**, 403 (1993).
25. B. V. Derjaguin, *Trans. Faraday Soc.*, **36**, 203 (1941).
26. J. N. Israelachvili and G. E. Adams, *J. Chem. Soc. Faraday Trans.*, **74**, 975 (1978).
27. V. E. Shubin and P. Kekicheff, *J. Colloid Interface Sci.*, **155**, 108 (1993).
28. J. L. Parker and H. K. Christenson, *J. Chem. Phys.*, **88**, 8013 (1988).
29. S. J. O'Shea, M. E. Welland and J. B. Pethica, *Chem. Phys. Lett*., **223**, 336 (1994).
30. B. V. Derjaguin, *Kolloid Z*., **69**, 155 (1934).
31. U. Hartmann, *Phys. Rev. B*, **43**, 2404 (1991).
32. J. N. Israelachivili, *Intermolecular & Surface Forces*, Academic Press, New York (1991).
33. H. Shin, M. Agarwal, M. R. de Guire and A. H. Heuer, *Acta Mater.*, **46**, 801 (1998).
34. E. J. W. Verwey and J. T. G. Overbeek, *Theory of the stability of lyophobic colloids*, Elsevier, New York (1948).
35. R. Hogg, T. W. Healy and D. W. Fuersten, *Trans. Faraday Soc*., **62**, 1638 (1966).
36. R. J. Hunter, *Foundations of colloid science*, Oxford University Press, Oxford, U.K. (1987).
37. D. Y. C. Chan, R. M. Pashley and L. R. White, *J. Colloid Interface Sci*., **77**, 283 (1980).
38. J. L. Parker, *Prog. Surf. Sci*., **47**, 205 (1994).
39. J.-W. Park and D. J. Ahn, *Colloids Surf. B: Biointerfaces*, **62**, 157 (2008).

40. W. A. Ducker, T. J. Senden and R. M. Pashley, *Nature*, **353**, 239 (1991).
41. R. G. Horn, D. T. Smith and W. Haller, *Chem. Phys. Lett*., **162**, 404 (1989).
42. J. Y. Choi and D. K. Kim, *J. Sol-Gel Sci. Technol.*, **15**, 231 (1999).
43. M. Schultz, St. Grimm and W. Burckhardt, *Solid State Ionics*, **63-35**, 18 (1991).
44. R. M. Pashley, *J. Colloid Interface Sci*., **83**, 531 (1981).
45. D. Rahmat, C. Muller, J. Barthelmes, G. Shahnaz, R. Martien and A. Bernkop-Schnurch, *Euro. J. Pharm. Biopharm*., **83**, 149 (2013).
46. M. Y. Lee, S. J. Park, K. Park, K. S. Kim, H. Lee and S. K. Hahn, *ACS Nano*, **5**, 6138 (2011).